OPTIMIZING THE THERMAL MANAGEMENT OF NSLS-II RF BPM ELECTRONICS*

B. Kosciuk#, M. Maggipinto, K. Vetter, BNL, Upton, NY 11973, USA

Abstract

The NSLS-II Synchrotron Light Source currently under construction at Brookhaven National Laboratory is expected to provide unprecedented orbit stability in order to fully utilize the very small emittance of the electron beam. The required sub-micron resolution and stability motivated the development of new state-of-the-art beam position monitoring (BPM) electronics. A fundamental aspect of the BPM system development leveraged the fact that dynamic thermal gradients are the dominant source of BPM position drift. The temperature dependent drift is predominantly introduced in the analog front end (AFE) electronics. Here we discuss the methods employed to enhance the heat transfer from the BPM AFE and their effects on overall performance of the BPM electronic systems.

MOTIVATION FOR THERMAL OPTIMIZATION

One of the most challenging aspects of sub-micron RF BPM design for 3rd generation light sources is the ability to provide a stable beam orbit on the order of a tenth of the beam emittance which typically translates to approximately 200nm. In order to achieve 200nm RMS stability, careful consideration of many aspects of the machine design is essential including, mechanical stability of BPM pickup supports, ground motion, and RF BPM electronics drift. In this report the RF BPM electronic drift is considered from the perspective that electronically induced beam motion results from a dominant dependence on time-dependent thermal dynamic induced gain variations.

The conceptual design philosophy of the NSLS-II RF BPM electronics considered the fact that independent RF receiver channel gain variations are dominated by dynamic thermal gradients. The required 200nm stability is typically specified on the order of several hours measured in bandwidths on the order of low KHz to Hz regime. For most electronic device technologies 1/f noise (i.e. flicker noise) dominates below a few KHz. Flicker noise extends down to the sub-hertz regime and manifests in the form of a random walk when observed in the temporal domain. Flicker noise and also Gaussian noise are related to temperature through a direct proportionality. As such, as the magnitude of the thermal dynamic gradients are reduced, also are the induced time-dependent gain fluctuations, and hence variations in reported beam position.

*Work supported by … DOE Contract No: DE-AC02-98CH10886
#bkosciuk@bnl.gov

To achieve long-term stability on the order of 200nm requires receiver channel-channel gain variations to be on the order of 10^{-5}. The NSLS-II RF BPM achieves the 200nm long-term stability goal by considering an overall system approach based on minimizing time-varying thermal dynamic influences. In order to maintain 200nm stability of the electronics the BPMs are housed in a ±0.1°C thermally regulated rack. Additionally, careful consideration to the RF board layout has been made to implement thermal elements to efficiently remove heat from thermally sensitive components such as RF amplifiers, and analog to digital converters (ADCs). The primary advantage of employing thermal management to achieve 200nm long-term stability is that no dynamic calibration signals are required thereby enabling observation and processing of raw beam signals with no artificially induced perturbations.

CONVECTIVE COOLING

Early in the development phase of the BPM electronics, the decision was made to avoid using local cooling of active components on the AFE such as the use of cooling fans typically seen on CPU chips. Studies had shown that such devices are a primary source of failure in other BPM electronic systems. However, finite element analysis of the ADC chip revealed that a significant drop in operating temperature could be realized by implementing a forced air cooling system found in commercially available actively cooled rack style electrical enclosures (see Fig 1).

Electronics installed in traditional racks typically rely on locally mounted convective fans within the electronics chassis to increase convection over components. Ultimately the heat generated by the electronics within the rack must be transferred via conduction through walls of the enclosure. The net effect of this is an operating temperature within the rack well above ambient. Fig 1 (a) shows the temperature distribution of the ADC with 2 watts of internal heat flux and a static film coefficient of 15 W/m^2-°C simulating the operating conditions of the AFE mounted in a traditional rack.

The motivation to utilize temperature controlled racks came from the fact that these systems are capable of maintaining the temperature within the enclosure to a stability of ±0.1°C with heat loads as high as 5 kW. [1] The cooling system employs an active heat exchanger coupled with a powerful convective fan to force air over the installed electronics, drastically increasing the film coefficient and thereby improving the overall efficiency of convective cooling. Fig 1 (b) shows the same ADC with 2 watts of internal heat flux but with a film

ISBN 978-3-95450-121-2

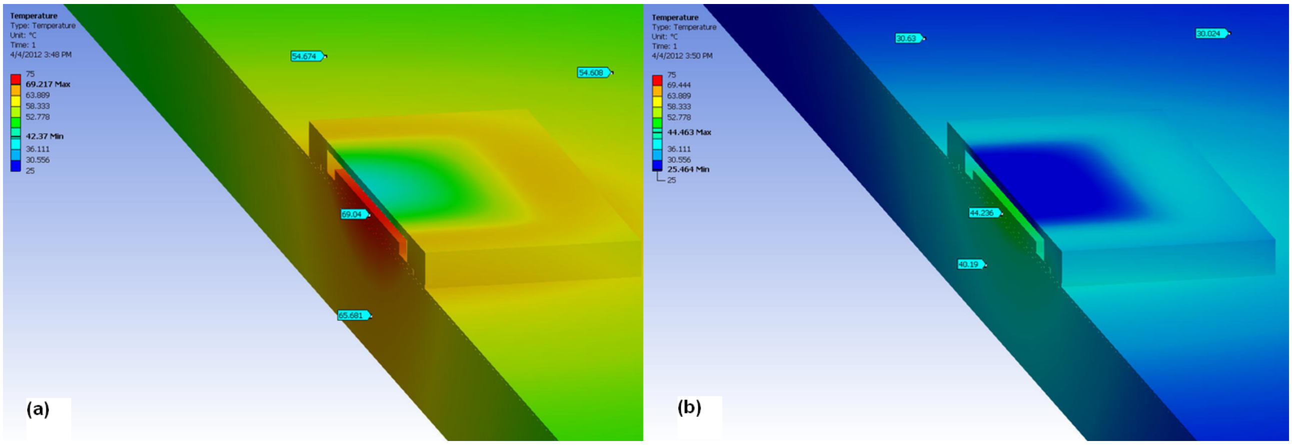

Figure 1: (a) Steady state temperature distribution of ADC chip in static air-free convection environment showing peak temperature of 69°C. (b) Same ADC chip in forced air environment simulating operating conditions of the thermally controlled rack. Peak temperature is reduced to 44°C.

coefficient of 100 W/m^2-°C. The resulting peak temperature of the ADC dropped from 69°C in the static case to 44°C in the case where active cooling was employed.

To further improve heat transfer from the ADC, a heat sink was added to the base of the AFE which provided a conductive path to the bottom plane of the aluminium chassis. On the underside of the FR4 board, directly beneath each of the four ADC chip, a small patch of solder mask was removed to allow the heat sink to contact the copper base (Fig 2). A Bergquist 5000S35 thermally conductive gap pad was used at the interface to insure good contact between the base of the board and the heat sink [2]. This material has a thermal conductivity of 5 W/m-K and readily conforms to uneven surfaces. Fig 3 shows the temperature distribution of the ADC with the same boundary conditions as the forced convection case in Fig 1(b) but with the addition of the heat sink. The peak temperature in this case dropped to 35°C, an improvement of 9°C.

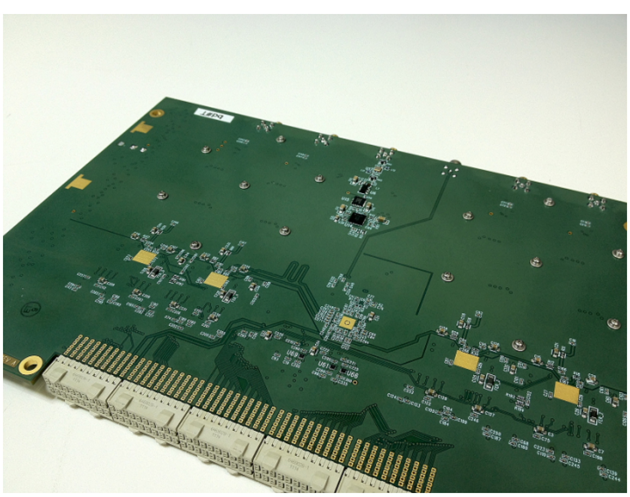

Figure 2: Underside of the AFE showing areas beneath the ADCs cleared of solder mask to thermally couple to heat sinks.

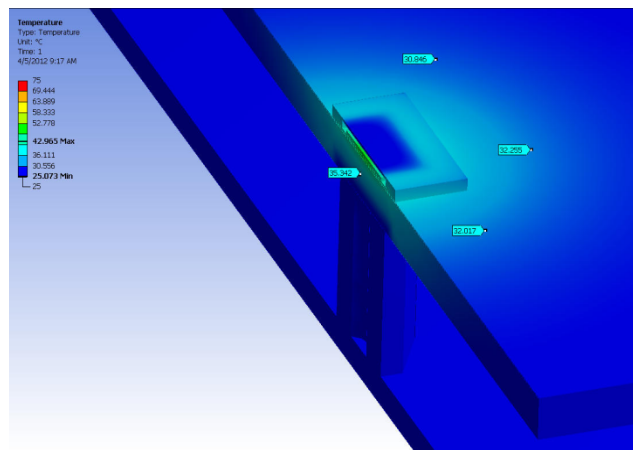

Figure 3: Temperature distribution of ADC with heat sink to bottom plane of chassis showing peak temperature of 35°C at the base of the ADC.

RF CAGES

In an effort to improve channel to channel isolation, specially designed aluminium RF cages were secured to the top of the AFE to minimize spatial RF coupling between adjacent channels. These RF cages proved to be somewhat effective at providing channel to channel isolation. However due to their proximity to the ADCs, it was decided to utilize the aluminium cage as an additional heat sink. The packaging design of the ADC was such that most of the internal heat generation would conduct directly to the board however it was felt that the additional conduction path to the RF cage could only benefit heat transfer. An extension was added to the design of the cage that would contact the top of the ADC package with thermal gap pad at the interface (Fig 4). Since forced air from the active cooling of the rack would pass over these cages, they would be an effective heat sink for any residual heat transferred into the packaging of the ADC.

ISBN 978-3-95450-121-2

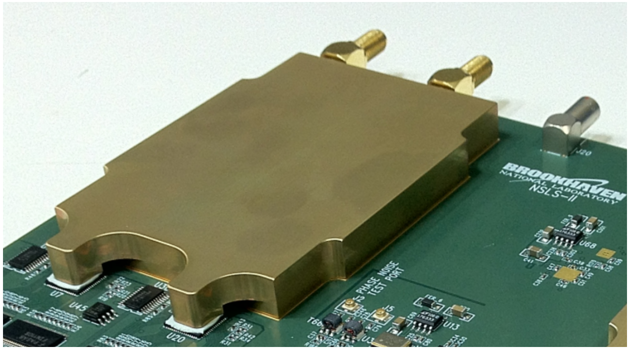

Figure 4: RF cage providing improved channel to channel isolation while providing additional heat sink for ADCs.

PERFORMANCE

Sensors integrated into the AFE board allowed temperature data to be collected over a long duration test. We installed eight BPMs into a temperature controlled rack and collected temperature data for each over a period of 60 hours.

Temperature stability was exceptional with RMS values ranging from 0.04°C to 0.14°C and peak to peak values ranging from 0.4°C to 1.3°C. The operating temperatures of the ADCs agreed well with the predicted value of 35°C (Fig 3) and ranged from 33.3°C to 37.8°C.

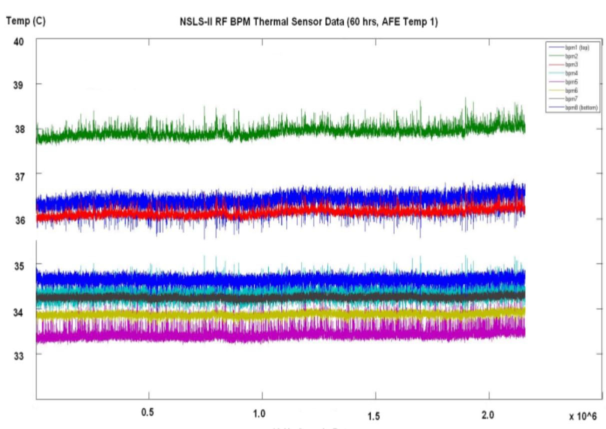

Figure 5: Long term temperature plot of 8 BPMs installed in a temperature controlled rack showing stability over a 60 hour period.

CONCLUSIONS

The temperature controlled racks proved to be very effective at stabilizing the operating temperature of the AFE which is critical to achieving the long term stability requirements for NSLS-II RF BPMs.

Incorporating heat sinks at the base of the ADC and modifying the RF cages to provide an additional heat sink to the top of the chip significantly lowered the operating temperature of the chip to 35°C.

Figure 5: Typical operational BPM rack configuration showing two racks with integrated temperature control on the right side.

REFERENCES

[1] K. Vetter, "NSLS-II RF Beam Position Monitor", BIW-2010, Santa Fe, May 2010, TUPSM037

[2] Datasheet "Gap Pad® 50000S35" manufactured by The Bergquist Company

ISBN 978-3-95450-121-2